Gold nanoparticles: effect of treatment on structure and catalytic activity of Au/Fe_2O_3 catalyst prepared by co-precipitation

D. Horváth [a], L. Toth [b] and L. Guczi [a,*]

[a] *Department of Surface Chemistry and Catalysis, Institute of Isotope and Surface Chemistry, CRC, HAS, PO Box 77, H-1525 Budapest, Hungary*
E-mail: guczi@alpha0.iki.kfki.hu
[b] *Institute of Technical Physics and Materials Science, PO Box 49, H-1525 Budapest, Hungary*

Received 29 January 2000; accepted 12 May 2000

1 wt% Au/Fe_2O_3 catalyst was prepared by a co-precipitation method. The structure of the sample in the as prepared, oxidized and reduced states was investigated by means of X-ray photoelectron spectroscopy (XPS), transition electron microscopy (TEM), electron diffraction (ED) and X-ray diffraction (XRD). The structure of the samples after various treatments and their activity in the CO oxidation were compared. The results show the stability of the gold particle size during the treatments. However, after oxidation, a slight shift in the Au 4f binding energy towards lower values points to the formation of an electron-rich state of the metallic gold particles compared to that revealed in the as prepared sample. Simultaneously, a goethite phase in the Fe_2O_3 support is present, which is not observed in the "as prepared" and reduced samples. In the reduced sample the presence of a crystalline maghemite-c phase indicates a change in the support morphology. In the CO oxidation the oxidized sample shows the highest activity and it might be the result of the cooperative effect of goethite, FeO and the electron-rich metallic gold nanoparticles. We suggest that a structural transformation occurs along the gold/support perimeter during the treatments and we propose a possible mechanism for the effect of the oxidation treatment.

Keywords: Au/Fe_2O_3 catalyst, structural study, CO oxidation, mechanism of the structural changes

1. Introduction

The low reactivity of gold is attributed to the completely filled 5d shell and the relatively high value of its first ionization potential [1]. As a result, gold has been used as an inert component in the platinum/gold foil as a model system applied in hydrocarbon catalysis [2,3]. Despite the available theoretical and practical evidence the gold was found to be active under certain conditions observed in the seventies [4].

It has well been established that the catalytic activity of gold can be governed by two factors: (i) the gold particle size being in the range 2–6 nm, and (ii) the nature of support. In the last decade gold appeared to be widely investigated and the result was excellently reviewed by Bond [5]. A wide range of reactions has also been studied on gold/support systems. Among the first studies Galvagno et al. investigated the gold activity in the O_2/H_2 [6–8] and in the NO/H_2 [9] reactions. Haruta et al. discovered that small gold particles supported on Co_3O_4, Fe_2O_3 and TiO_2, had high activity in the CO and H_2 oxidation [10,11], NO reduction [12], CO_2 hydrogenation [13] and in the catalytic combustion of methanol [14]. Andreeva et al. investigated the water–gas shift reaction [15]. These studies pointed out that the reactivity of gold was attributable mainly to the small particle size and to the metal/support interaction.

From these experiments it has appeared that the main feature in preparing active gold catalysts is the way in which the deposition of the gold precursor on the support occurs. One of the major factors in the deposition–precipitation technique is the appropriate pH value [16]. Some recently developed methods, like arc-melting, chemical vapor deposition (CVD), co-sputtering [17] and pulsed laser deposition (PLD) [18] also led to good results.

Despite the wide knowledge about the adequate preparation technique to produce a highly active gold catalyst, there are many open questions to be answered. One of these is the stabilization of small gold particles inserted into the zeolite supercage [19–21]. In these studies Fraissard showed the presence of $Au^{\delta+}$ species by ^{129}Xe NMR and DRIFT studies [21]. Ichikawa also prepared positively charged gold particles encapsulated in NaY zeolite and observed higher activity than that shown by metallic gold particles [22].

However, in recent structural studies on gold particles deposited on $Mg(OH)_2$, Haruta showed that below and above 1 nm size the gold particles exist in icosahedral and in fcc cubooctahedral symmetry, respectively [23]. This fact proved the importance of geometrical symmetry in developing highly active gold catalysts. On the $Au/Mg(OH)_2$ samples positively charged $Au^{\delta+}$ species were also observed by Mössbauer spectroscopy [24]. Galvagno et al. arrived at a similar conclusion, which also suggested the importance of Au^{+} and Au^{3+} species in the case of Au/Fe_2O_3 catalysts [25,26]. From these experiments it is now obvious that the gold particle size is of primary importance, but its critical size depends on the support (for MgO it is <1 nm, whereas for TiO_2, Fe_2O_3 the size is <10 nm).

* To whom correspondence should be addressed.

Model studies also supported that the major factor in determining catalytic activity in CO oxidation is the size of gold particles. According to the work carried out by Goodman et al. [27], the maximum in activity is measured on Au/TiO_2 having 4 nm gold particles. Below this size the band gap abruptly increases and gold loses its metallic character. Similar statement was done in our previous study on a $Au/FeO_x/SiO_2/Si(100)$ model system [28] with low gold loading prepared by pulsed laser deposition. A promoting effect of iron oxide on the catalytic activity of gold nanoparticles was also established. We found the three factors operate simultaneously to control the activity of the gold system: (i) small metallic gold particles, (ii) amorphous iron oxide support, and (iii) oxygen vacancies caused by the change of the valence state of iron.

In most of the earlier works the supported gold samples were calcined and the increasing calcination temperatures increased the catalytic activity. Here the effect was explained by a change in the gold particles size morphology from spherical to hemispherical [29]. In contrast, Park and Lee [30] showed the opposite effect on Au/TiO_2, and Au/Fe_2O_3 samples. XPS and XAFS studies showed that increasing calcination temperature gave rise to the fraction of metallic gold in the phase transition of $Au(OH)_3$ through Au_2O_3 to metallic gold. Since it was suggested that Au^+ were the active site for the CO oxidation, the deactivation by calcination was due to the formation of metallic gold particles.

Lin et al. found that even the drying conditions (vacuum vs. oven drying) changed the oxidation state and morphology of the gold particles [29]. High-temperature reduction/calcination followed by low-temperature reduction gave the highest activity, which was correlated with the enhanced proportion of metallic gold. In contrast, Gupta et al. observed a transfer from Au/Fe_2O_3 to Au/Fe_3O_4 during hydrogen treatment and a simultaneous reduced rate in the CO oxidation [31,32]. A similar effect was reported by Haruta et al. on preoxidized Au/TiO_2 samples [33]. On the other hand, Baiker found gold in metallic state after colloidal gold deposition on TiO_2 and ZrO_2 and the Au/ZrO_2 sample could be activated by calcination and the presence of the positively polarized gold sites was identified by FTIR [34].

Notwithstanding the widening research on gold catalysts, still numerous conflicting pieces of evidence are available about the effect of treatments, such as the oxidation state of gold and the effect of support. In the present paper we use the same pretreatments on the 1 wt% Au/Fe_2O_3 catalyst prepared by co-precipitation as were applied previously on the model system [28]. We use XPS, TEM, XRD and other techniques to study the effect of various treatments on the structure and morphology of the gold particles, on the iron oxide support and the metal/support interaction. CO oxidation as test reaction is employed to correlate the structural changes to the catalytic activity.

2. Experimental

2.1. Catalyst preparation

The catalyst was prepared by a co-precipitation method using $HAuCl_4$ and $Fe(NO_3)_3{\cdot}9H_2O$. The aqueous solution of the components (60 ml) was added into a 1 M aqueous solution (400 ml) of Na_2CO_3 at a rate of 7.5 $cm^3\,min^{-1}$ at 75 °C under vigorous stirring [26]. The co-precipitate was digesting in the mother solution at 77 °C for 18 h washed several times with hot water and dried at 80 °C for three days. The sample was ground and meshed. The fraction in 0.1–0.3 mm diameter range was selected for the investigations. The final gold loading being 0.94 wt% was determined by prompt gamma spectroscopy (PGS) [35].

2.2. Catalyst characterization

2.2.1. X-ray photoelectron spectroscopy (XPS)

Chemical states of the constituents as well as electronic structure of the catalysts were investigated by the core level spectra in a photoelectron spectrometer type KRATOS XSAM 800. For chemical analysis the core level electrons were excited by Al K_α radiation. The spectra were taken by FAT mode and the carbon peaks were used as binding energy reference. After having used the samples in the CO oxidation, their surface composition was also determined. The spectra of the Fe 2p core level electrons were fitted with Gaussian–Lorentzian product peaks after Shirley background subtraction, while for the evaluation of other peaks a linear background subtraction was used.

The Au $4f_{7/2}$, Fe 2p and O 1s photoelectron lines in the Au/Fe_2O_3 samples in the "as received" state, after oxidation and reduction were determined in an *in situ* reaction chamber directly attached to the spectrometer. The same pretreatment conditions were applied before catalytic measurements. The pure support was also investigated in the same way.

2.2.2. Transmission electron spectroscopy (TEM)

Before and after pretreatments the microstructure and morphology of the samples were determined by transmission electron microscopy (TEM) using a Philips CM-20 type microscope. The morphology of the sample was investigated by plan-view imaging. The sample was pretreated using the same conditions as were applied for XPS and catalytic measurements. The electron diffraction pattern was also established in the different stages of the pretreatment.

2.2.3. X-ray diffraction (XRD) measurements

X-ray diffraction measurements were carried out in a Philips X-ray diffractometer equipped with a Cu K_α source using a Guinier camera. The as prepared and the differently pretreated gold-containing samples as well as the pure support were investigated.

2.3. Catalytic measurements

The CO oxidation was applied as catalytic test reaction. The reaction has a well known mechanism on several supported metal surfaces like Pt [36], Pd [37] and in recent years a great deal of experiments were made using supported gold catalysts [38–40].

The reaction was carried out in an all glass made circulation reactor linked to a mass spectrometer via a capillary leak to ensure viscous flow. The change in the CO and CO_2 concentrations as a function of time was followed using the same total pressure in the reactor. Due to the sampling device the amount of CO_2 was measured at a standard 180 mbar pressure monitoring the $m/e = 44$ peak intensity. In each measurement the composition of the gas mixture was 10 mbar CO, 10 mbar O_2 and 180 mbar He, which were mixed and introduced into the reactor and due to the volume increase, the total pressure became 180 mbar. The CO oxidation was performed on the as prepared, oxidized and reduced samples. Calcination in oxygen was carried out in 150 mbar O_2 at 200 °C for 1 h. Reduction took place in 150 mbar hydrogen at 200 °C for 1 h using the calcined sample. The reactions were usually performed at 50 °C. Since the pure Fe_2O_3 support might also have catalytic activity in the CO oxidation, the reaction was also measured on the support itself in preliminary experiments at somewhat higher temperature.

A preliminary calibration was performed to calculate the amount of CO_2 formed. In separate experiments the intensity–CO_2 pressure relationship was determined at 180 mbar total pressure and this was used for quantitative evaluation of the amount of CO_2. In the actual measurement the intensity of the $m/e = 44$ peak after background subtraction was determined. Under the conditions used for the CO oxidation, 0.3 μmol CO_2 in the gas phase corresponds to 100% CO conversion.

3. Results

3.1. X-ray photoelectron spectroscopy (XPS)

The positions of the Fe 2p, Au $4f_{7/2}$ and O 1s peaks after different treatments were measured by means of XPS. In figure 1 the Fe 2p core level spectra are plotted in the as prepared, oxidized and reduced state. The binding energy in the as prepared and the oxidized samples (curves (a) and (b)) lies at 711 and 710.9 eV, respectively, indicating the presence of Fe_2O_3 and/or FeO(OH) species. After reduction (curve (c)) the peak shifted toward 710.2 eV which shows the presence of FeO and/or Fe_3O_4. These changes in the position of Fe 2p peak cannot be observed in the pure Fe_2O_3 sample treated under the same conditions (the binding energies appeared at 711.2–711.4 eV, the values being indicative of Fe_2O_3 and/or FeO(OH)).

Figure 2 shows the gold Au $4f_{7/2}$ peak in the as prepared state with 84.3 eV BE being characteristic of metallic gold (curve (a)). A slight shift towards lower binding energy

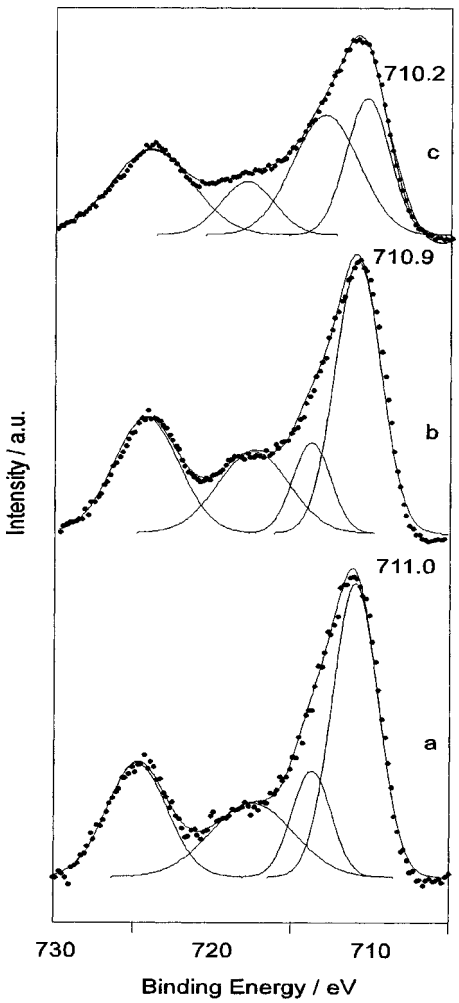

Figure 1. XPS spectra of the Fe 2p peak at different stages of treatment: (a) as prepared, (b) oxidized and (c) reduced.

is observed after oxidation, the BE being 83.9 eV for the $4f_{7/2}$ peak (curve (b)). After reduction (curve (c)) the BE value does not change (83.8 eV). These values indicate metallic state for gold even after oxidation. We have to note that the gold signal is weak which makes curve fitting difficult.

In figure 3 the O 1s enveloping curve is asymmetric towards the higher binding energy region which indicates the presence of different oxygen species in the sample. In the as prepared sample (curve (a)) the main component lies at 530.3 eV which can be assigned to Fe_2O_3 phase, which after treatments shifted to 529.6–529.7 eV corresponding to FeO (curves (b) and (c)). The second component of the asymmetric peak is found at 533.5 eV BE (curve (a)), which is most likely attributed to adsorbed water on the surface. After oxidation (curve (b)) this peak disappeared and two new lines could be recorded at 531.1 and 535.2 eV. After reduction the former peak retained its position near this value at 531.3 eV which is assigned to OH bond (curve (c)). However, the latter is shifted to 534.1 eV which is assigned to adsorbed water on the surface. The position of the O 1s peak at 535.2 eV BE is rather uncertain and hard to identify

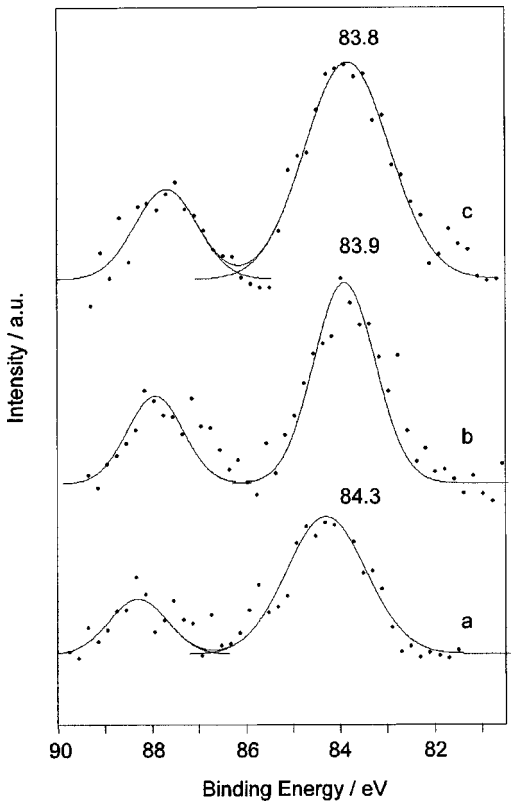

Figure 2. XPS spectra of the Au 4f peak at different stages of treatment: (a) as prepared, (b) oxidized and (c) reduced.

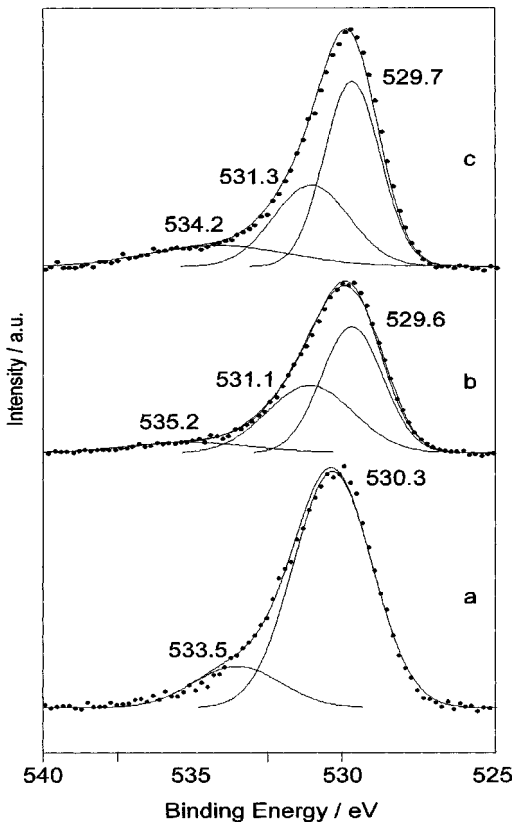

Figure 3. XPS spectra of the O 1s peak at different stages of treatment: (a) as prepared, (b) oxidized and (c) reduced.

in the absence of any available reference data. A possible assignation can be O_2^- species.

3.2. Transmission electron microscopy (TEM)

Owing to the scarcely distributed gold particles (which is a consequence of the low gold concentration at the surface) the TEM technique is rather troublesome and time consuming to find areas with sufficient amount of gold particles. Nevertheless, figure 4 shows the TEM images after the various treatments, the size of metallic gold particles being in the range of 7.5–12.5 nm. The size of the gold particles does not change significantly due to the pretreatments as shown by the size distribution histograms (figure 5).

According to the electron diffraction patterns of the as prepared and reduced samples the diffraction lines show only a Fe_2O_3 phase, while in the oxidized sample a new phase which is assigned to FeO(OH) also appears (figure 6). The lines appeared at $d = 2.585$, 2.453 and 1.805 Å separately, while the literature data for spacing of the goethite (021), (111) and (211) reflexions are $d = 2.583$, 2.450 and 1.802 Å, respectively.

3.3. X-ray diffraction measurements

In figure 7 the XRD spectra also indicate phase transitions in the iron oxide support due to the pretreatments. The spectrum of the as prepared sample (curve (b)) shows only the peaks of a Fe_2O_3 hematite phase, which is the same as in the case of the pure support (curve (a)) except that the intensities of the peaks are diminished. For the reduced sample (curve (d)) the peaks of Fe_2O_3 are indicative of the maghemite-c phase appeared at $2\theta = 45.5°$, 66.4°, 77° and 84° next to the hematite lines. In the oxidized state (curve (c)) only the peaks of the hematite phase can be observed, however, their intensity decreased significantly compared to the as prepared sample.

The peaks characteristic of gold could not be observed in any spectra, which is surprising because the particles, sizing 7.5–12.5 nm and detected by TEM, ought to be seen by XRD. The possible reason is as follows. The phase concentration of the gold particles should be in the range of 4–5% in the area "seen" by the X-ray which condition is obviously not fulfilled. On the other hand, the visibility of an electron diffraction pattern in a TEM measurement is due to the fact that the electron beam is already focussed to the area in which larger amounts of Au particles exist.

3.4. CO oxidation

In figure 8(a) a preliminary experiment is presented on the CO oxidation carried out at 100 °C over oxidized 0.3 wt% Au/Fe_2O_3 and Fe_2O_3 samples. The preparation method and the pretreatment of these samples are the same as those described in section 2 for the 1% Au/Fe_2O_3 sample. Similarly to the model catalyst systems, in which $Fe_2O_3/SiO_2/Si(100)$ and $Au/Fe_2O_3/SiO_2/Si(100)$ samples

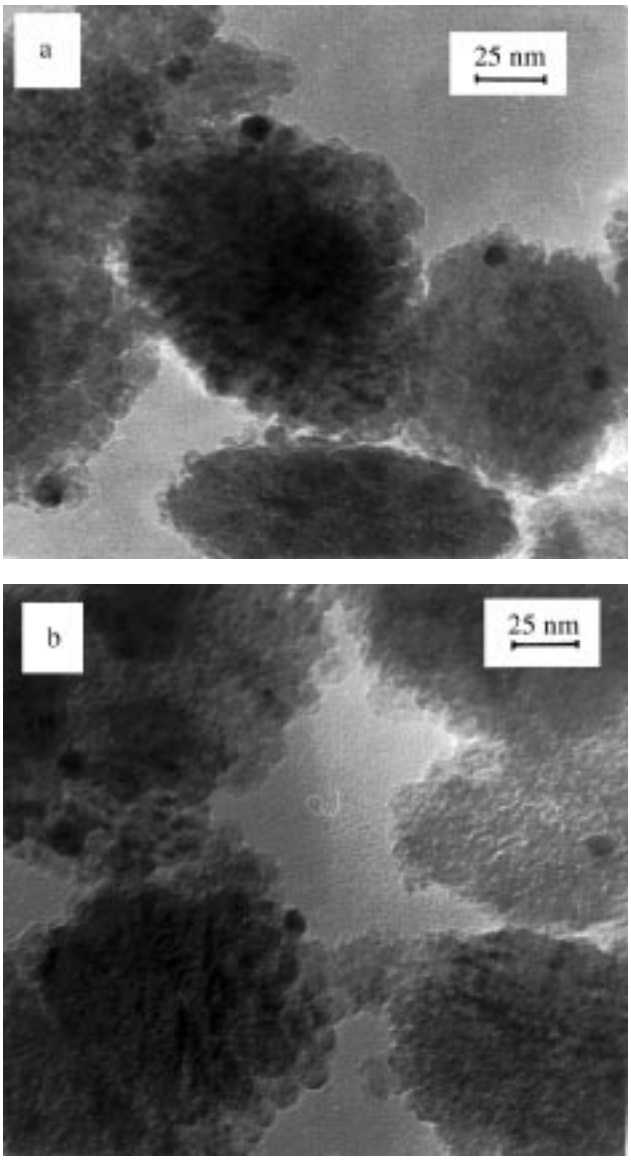

Figure 4. TEM images of the 1% Au/FeO_x sample at different stages of treatment: (a) as prepared, (b) oxidized and (c) reduced.

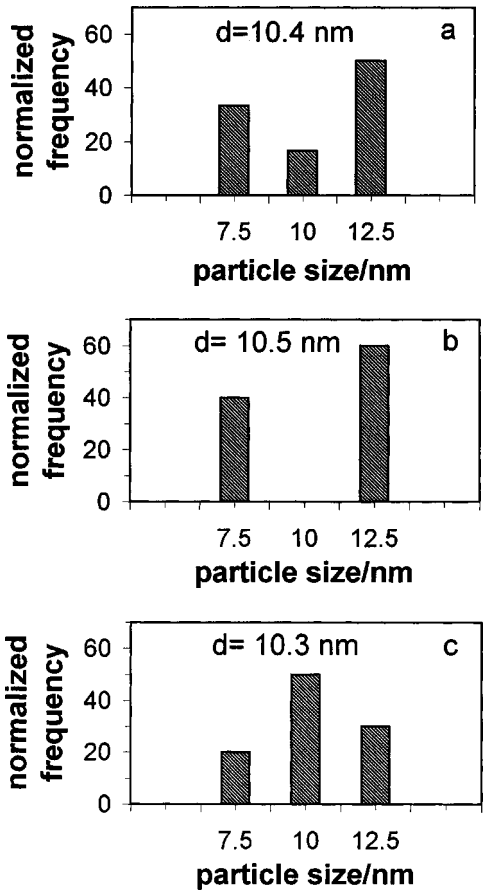

Figure 5. Size distribution diagrams of the Au particles on the differently treated samples: (a) as prepared, (b) oxidized and (c) reduced.

were compared [28], the initial rate of the CO oxidation was significantly higher on a pretreated Au/Fe_2O_3 than on the pure Fe_2O_3 sample ($r_0 = 0.1\ \mu\text{mol}\,\text{mg}_{\text{cat}}^{-1}\,\text{min}^{-1}$ and $r_0 = 5.1 \times 10^{-3}\ \mu\text{mol}\,\text{mg}_{\text{cat}}^{-1}\,\text{min}^{-1}$, respectively).

The effect of treatment was performed over 0.1 g of the 1 wt% Au/Fe_2O_3 sample under the same conditions at 50 °C. Based on the catalytic investigations the initial reaction rate (r_0) of the CO_2 formation was always evaluated. Using the n_{CO_2}–time plots, from the equation of the fitted curves r_0 was always determined as the slope of the kinetic curve extrapolated to zero time.

In figure 9 the as prepared sample shows a very low, nearly negligible activity ($r_0 = 9 \times 10^{-4}\ \mu\text{mol}\,\text{mg}_{\text{cat}}^{-1}\,\text{min}^{-1}$). After oxidation of the sample the activity in the CO oxidation increased by two orders of magnitude and shows the highest value among the samples investigated ($r_0 = 0.11\ \mu\text{mol}\,\text{mg}_{\text{cat}}^{-1}\,\text{min}^{-1}$). Subsequent reduction after oxidation caused a decrease in the activity compared to the value of the oxidized sample, although the activity of the reduced sample remains higher than the value of the as prepared sample ($r_0 = 7.1 \times 10^{-2}\ \mu\text{mol}\,\text{mg}_{\text{cat}}^{-1}\,\text{min}^{-1}$).

On the pure support investigated under the same conditions as in case of the presence of gold the activity was one order of magnitude lower than that measured on the least active as prepared sample.

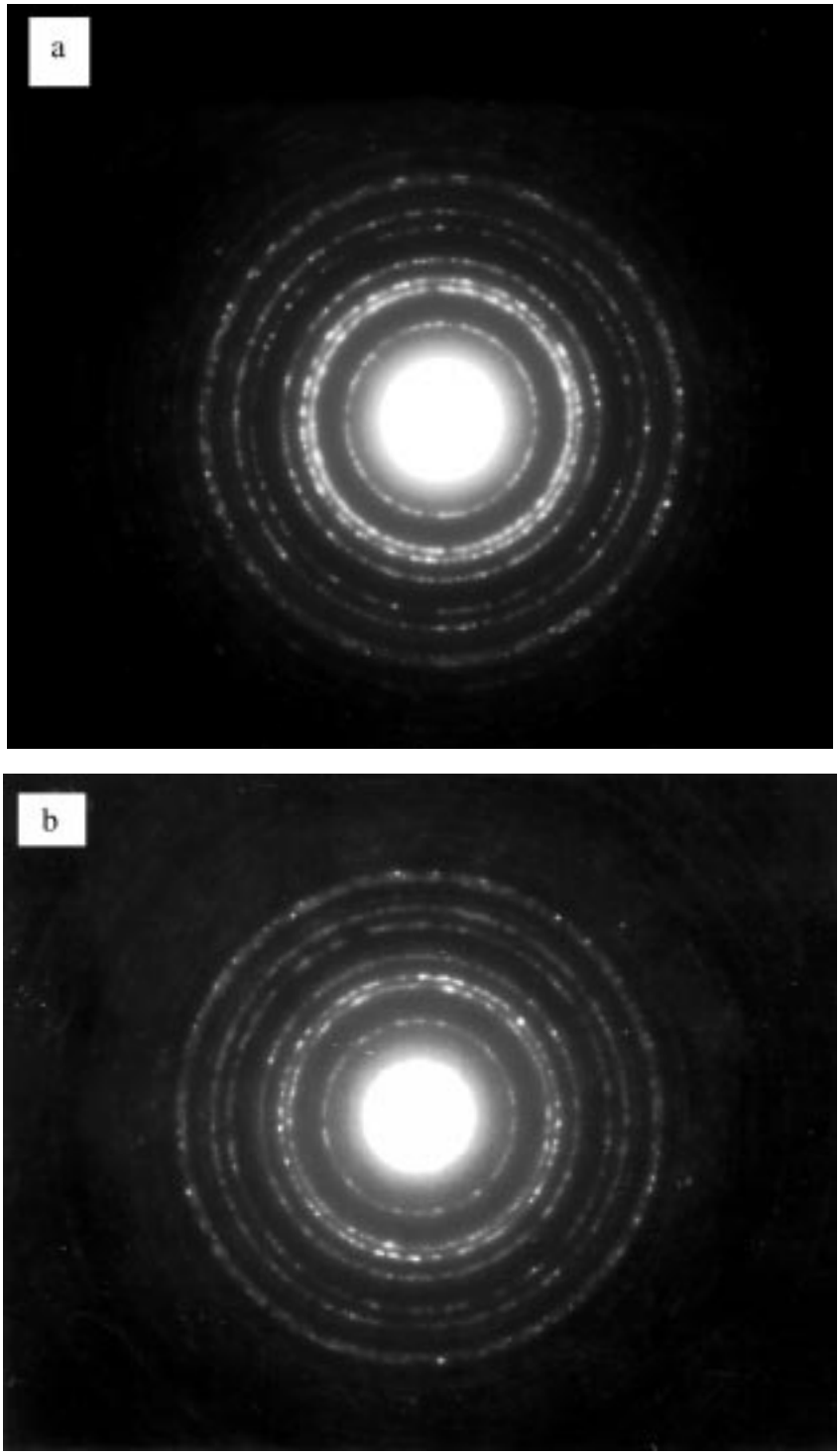

Figure 6. Electron diffraction patterns of the differently treated samples: (a) as prepared sample with the lines of Fe_2O_3, (b) reduced sample with the lines of Fe_2O_3 and (c) oxidized sample indicating the lines of the goethite.

4. Discussion

The results presented here are in good agreement with our previous finding [28], i.e., the nanoscale gold particles are active in the CO oxidation and the gold maintains its metallic state, even after several treatments. On the other hand, during the development of high catalytic activity the structure of Fe_2O_3 must be changed [28]. These findings are based on the study of model catalysts in which we have suggested the promoting effect of iron oxide on the activity of the gold nanoparticles. As was indicated, the gold particles in metallic state are stabilized by iron oxide even at low gold loading and at small particle size. When

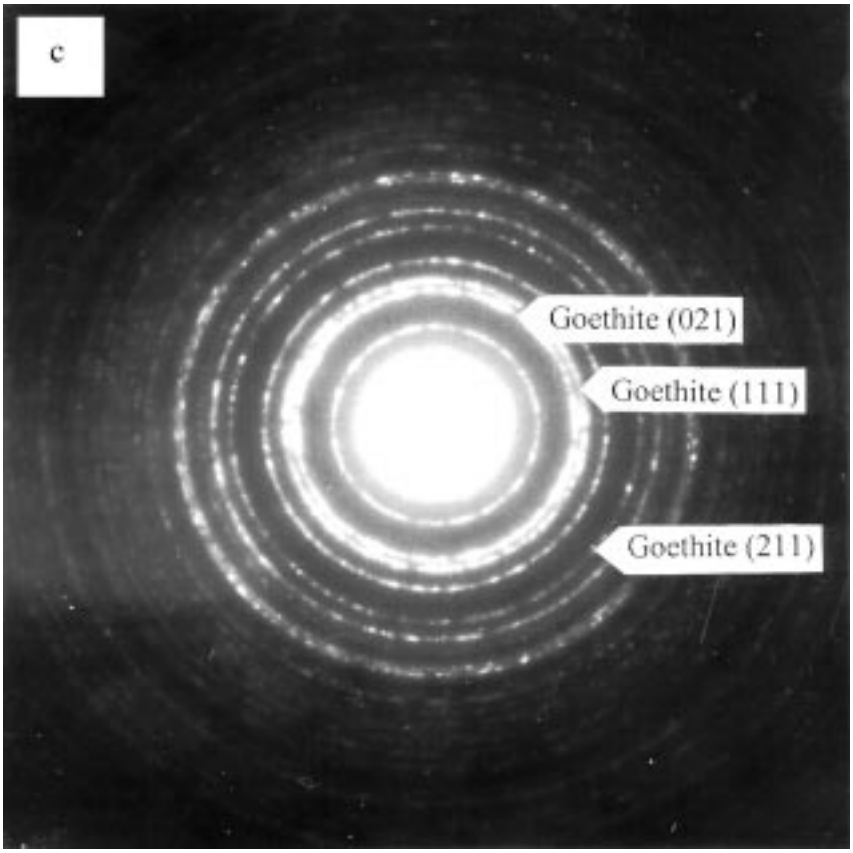

Figure 6. (Continued.)

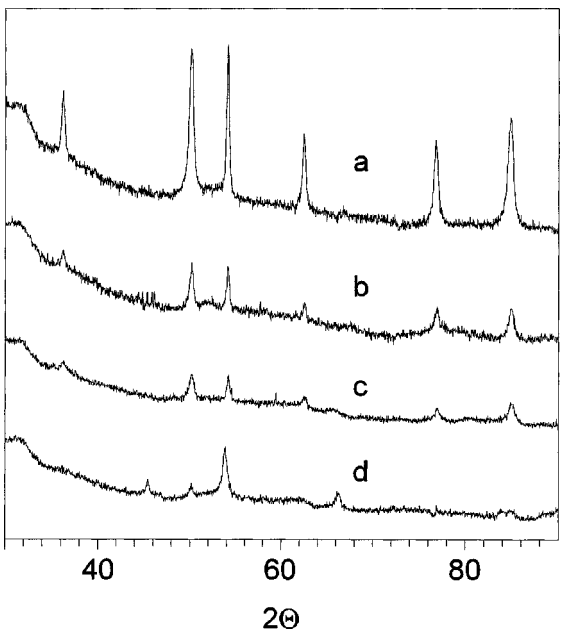

Figure 7. XRD spectra of the 1% Au/FeO_x samples and the pure support: (a) Fe_2O_3 support, (b) 1% Au/Fe_2O_3 as prepared, (c) 1% Au/Fe_2O_3 oxidized and (d) 1% Au/Fe_2O_3 reduced.

iron oxide becomes amorphous, interactions exist between the iron oxide and gold particles which are prerequisite for high activity. In addition, the structure and oxidation state of iron in Fe_2O_3 are also altered.

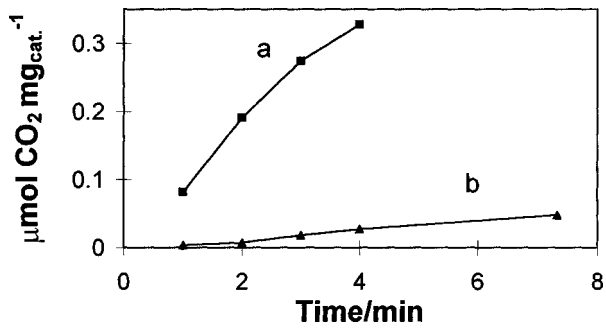

Figure 8. Preliminary experiment on the CO_2 formation at 100 °C after the oxidation treatment: (a) 0.3% Au/FeO_x and (b) pure Fe_2O_3 support.

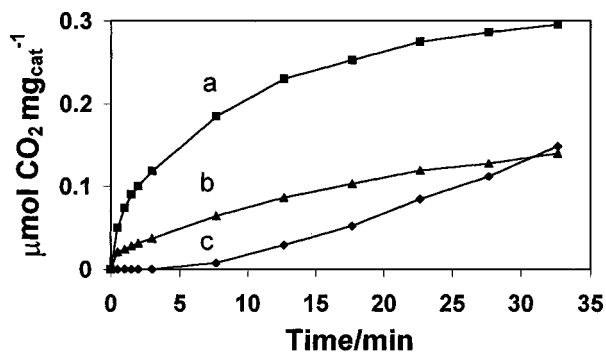

Figure 9. CO_2 formation at 50 °C on the 1% Au/FeO_x catalyst at the different stages of treatment: (a) oxidized sample, (b) reduced sample and (c) as prepared sample.

Table 1
Binding energy values (eV) with the indication of the possible states of the catalyst and the surface concentration of gold on 1% Au/FeO_x catalyst based on XPS investigation.

	Fe 2p (eV)	O 1s (eV)	Au 4f (eV)	Au (wt%)	Au/Fe $\times 100$
As prepared	711 FeO(OH) Fe_2O_3	530.3 Fe_2O_3 533.5 H_2O	84.3 Au^0	0.31	1.16
Oxidized	710.9 FeO(OH) Fe_2O_3	529.6 FeO 531.1 OH 535.2 O_2^-?	83.9 Au^0	0.34	0.98
Reduced	710.2 Fe_3O_4 FeO	529.7 FeO 531.3 OH 534.16 H_2O	83.8 Au^0	0.28	0.86

In the Au/Fe_2O_3 system XPS investigations indicate no structural transformation on the pure iron oxide support, which fact proves its stability before and after treatments carried out at 200 °C. Regardless of the treatment in He or O_2 only water was desorbed monitored by thermogravimetric analysis. The Fe 2p peaks appeared at 711.2–711.4 eV BE, which shows the presence of Fe_2O_3 and/or FeO(OH) of the support. Pure iron oxide showed negligible activity in the CO oxidation. Nevertheless, in the heat treatment the water may result both from adsorbed water and FeO(OH).

When the Au/Fe_2O_3 sample was studied in the as prepared state, the core level spectra for Fe 2p had similar features as that measured on the pure support. This points to an identical initial composition of the Fe_2O_3 in both cases. In accordance with other authors [22,41,42], in the as prepared sample the 711 eV BE recorded for the Fe 2p peak, shows the presence either of Fe_2O_3 or FeO(OH) phases, whose binding energies are very close to each other. The satellite peak at around 719 eV BE, however, unambiguously points to the presence of Fe^{3+} ions in the sample. Moreover, the O 1s peak measured at 530.3 eV BE also shows the presence of iron in the form of Fe_2O_3. The second component of the O 1s peak at 533.5 eV is likely due to the water adsorbed on the surface.

After oxidation both the Fe 2p and the satellite peaks remained nearly at the same position (710.9 and 719 eV, respectively) as they were in the as prepared sample. However, the O 1s peak was shifted towards 529.6 eV BE, which could be a result of the presence of FeO surface species formed after heat treatment. The second component of the O 1s peak at 531.1 eV was assigned to the presence of an OH bond which was still present in the form of FeO(OH) [42]. Surprisingly, a weak O 1s signal as a third component was also recorded at around 535.2 eV. In the absence of any reference data concerning such a high binding energy value of the O 1s peak, the exact identification of this peak is not available. Only some examples are known concerning this high binding energy for O 1s, which are around 533–534 eV. A similar binding energy for O 1s was identified for P_2O_5, B_2O_3 as well as SiO_2. For a $Fe_{40}Ni_{40}B_{20}$ amorphous ribbon the O 1s line measured at 532 eV BE was assigned to boron oxide species [43]. In addition to this, a value of 531.5 eV BE was also identified and was suggested as weakly bonded oxygen species at the iron/boron interface. Also a high value for O 1s species (534.6 eV) was observed on palladium and was devoted to particularly active oxygen species in the total combustion of m-xylene [44]. Based on Sanderson's calculations [45] and Nefedov's XPS experiments [46], Bielanski established [47] that the higher the value of BE, the lower is the electron density on the oxygen. In the oxides he referred to, the oxygen had a very low negative charge (-0.13, -0.23) which explained the high BE value for O 1s. Consequently, in our case oxygen species must be present whose electron density according to this principle is low (discussed later).

After reduction the Fe 2p peak showed a significant shift toward lower BE which appeared at 710.2 eV. This showed the presence of Fe_3O_4 in the iron oxide and the O 1s peaks at 529.7 and 531.3 eV indicated the presence of FeO and OH species, respectively. Both the characteristic satellite peak of Fe^{3+} and the very weak signal at 535.2 eV BE disappeared.

In table 1 data obtained by XPS are summarized. Here we show also the surface concentration of gold and the surface Au/Fe ratio. The species identified for iron and oxygen are already discussed. From table 1 it appears that gold remains in the metallic state and only slight changes can be seen in the BE. The small, but definite decrease in the Au $4f_{7/2}$ BE after oxidation is likely due to a change in the electron state of gold. There is a simultaneous decrease in the Au/Fe ratio. From the TEM investigations we know that the size of the gold particles did not change significantly during the various treatments. The decrease in the Au/Fe ratio means that after oxidation the FeO_x species migrate on top of the gold surface and partially cover it. We have to note here that the amount of gold observed by XPS is about one third of the real gold content in the catalyst sample.

TEM images showed a more or less homogeneous size distribution of the gold particles. Because of the low gold content on the catalyst, only a few metal particles are visible. The size of the gold particles lies in the range of 7.5–12.5 nm. The diameter of the Au particles does not change after the different treatments, which suggests the

secondary importance of the diameter of gold particles in revealing high catalytic activity.

Electron diffraction patterns show a number of diffraction lines and since the gold and the different FeO_x lines are overlapped, it is difficult to have an exact evaluation based on these measurements. The electron diffraction lines of different Fe_2O_3 phases show a definite change in the structure of the support, namely, in the oxidized state the three lines unambiguously prove the presence of FeO(OH) in the orthorhombic form called goethite.

The structural transformation in the support during the treatments was measured also by XRD. While the as prepared sample contains only hematite, which is the rhombohedral form of Fe_2O_3, in the spectrum of the reduced sample the maghemite-c lines indicate the presence of the cubic form of Fe_2O_3. The oxidized sample shows a somewhat amorphous state as the intensities of the hematite lines decreased compared to that of the as prepared sample.

Along with the XPS results these findings suggest that phase transitions occur on the support during the treatments starting from the Fe^{3+} ions through an amorphous phase, containing Fe^{2+} and Fe^{3+} ions, to maghemite-c- and hematite-containing phases. These results show remarkable agreement with our previous findings in the investigation of a model catalyst prepared by PLD [28].

The activity of the samples in the CO oxidation significantly changed after different treatments. Among the samples the oxidized form was the most active and its activity was one and half and two orders of magnitude higher (TOF $= 0.35\ s^{-1}$) than that measured on the reduced catalyst (TOF $= 0.22\ s^{-1}$) and on the as prepared sample (TOF $= 0.003\ s^{-1}$), respectively. This change in the activity cannot be attributed to the change in the surface carbon contamination, which is always present. A small increase in the activity could appear because of the decrease in the initial carbon concentration from 18.2 to 7.7 at% measured by XPS. The subsequent reduction treatment after oxidation made only a minute decrease in the carbon contamination (7.2 at%), while the activity in CO oxidation decreased to a much larger extent. So, we could not exclude the effect of carbon contamination, but this effect does not play a decisive role in creation of the catalytic activity.

In spite of the low initial reaction rate on the as prepared sample, after 30 min the CO conversion increases to a level measured on the reduced sample. This possibly indicates some transformations of the catalyst during the reaction.

After the complete catalytic cycles on the as prepared, oxidized and reduced samples, further oxidation caused reactivation of the sample to the level characteristic of that measured after the first oxidation treatment. This effect can be seen even after several catalytic cycles followed by reoxidation treatment, which proves either the unimportance of the surface carbon concentration in the reduced sample or the presence of active sites being reactivated after oxidation treatment.

Mechanism of the oxidation treatment on Au/Fe_2O_3 sample

Based on our present work and on our previous results on a model catalyst [28], we propose a possible mechanism for the effect of the oxidation treatment to reach the highest activity among the samples investigated. The scenario also explains the type of electronic interaction that occurs between the iron oxide support and the gold nanoparticles which helps the gold to maintain its metallic state and to increase catalytic activity.

In our previous paper we showed a shift of about 1 eV in the Au 5d valence band on the Au/SiO_2/Si(100) surface due to the size reduction resulting in $Au^{\delta+}$ species. This is in agreement with the results obtained for Cu and Ag nanoparticles, and it points to a strong interaction with the support [18]. We also showed a stabilization effect of the iron oxide layer in Au/FeO_x/SiO_2/Si(100) on the valence band structure of the Au particles by which the gold remains in metallic state even at a very low Au/Fe ratio. Our results presented here, show a similar effect of iron oxide on the gold nanoparticles. Nevertheless, the structure and oxidation state of iron are changed during the treatments.

In order to suggest a possible mechanism for the effect of treatment the following facts must be taken into consideration. (i) If the support is treated alone (without gold) there are no changes, neither in the core level binding energies of Fe_2O_3, nor in the catalytic activity revealed in the CO oxidation. (ii) If helium is used in place of O_2 to heat up the Au/Fe_2O_3 sample no increase in catalytic activity was experienced in the CO oxidation, although in both cases H_2O from FeO(OH) evolved leaving oxygen vacanceis behind on the surface. That is, in both cases metallic gold–vacancy pairs are generated. (iii) The size of the gold particles is not of primary importance in the catalytic activity as the catalytic activity did not change in parallel with the diameter of the gold particles.

The change in the structure of the iron oxide support and in the respective alteration in the core level electron properties must be assigned to the presence of the gold particles. This is because we could not observe any shifts in the binding energy of the Fe 2p peaks on pure support after the same treatments and there was only negligible catalytic activity of the pure Fe_2O_3. This effect is a consequence of the interface created during the treatment along the Au/Fe_2O_3 perimeter. This has been established by several authors, e.g., on the Au/TiO_2 system in which the decoration of gold particles by TiO_x species plays an important role [48].

Our results show that in the case of the as prepared sample we have metallic Au particles and the support consists of Fe_2O_3 and FeO(OH). After oxidation, surface Fe^{2+} ions along the Au/Fe_2O_3 perimeter were observed and a new O 1s peak appeared at 535.2 eV BE. This O 1s peak is considered not to originate from a lattice oxygen, but from a gas phase O_2 molecule whose s electrons are in a highly positively charged neighborhood.

Based on these findings a suggested mechanism for the effect of the oxidation treatment is as follows. During oxidation the FeO(OH) species on the surface at the gold/iron oxide interface (perimeter) are transformed into FeO species according to the following equations:

$$4\mathrm{FeO(OH)} \rightarrow 4\mathrm{FeO} + \square + 2\mathrm{H_2O_{(g)}} + \mathrm{O_{2(g)}} \quad (1)$$

$$\mathrm{Fe^{2+}} + \square + \mathrm{O_{2(g)}} \rightleftharpoons \mathrm{Fe^{3+}} + \mathrm{O^-_{2(s)}} \quad (2)$$

where $\square$ means an oxygen vacancy on the surface. One assumes that reaction (1) does not require an oxidative atmosphere because the heat treatment of the sample is sufficient to remove water. However, as we have mentioned, the experiment carried out on the same sample by heating it in He did not show phase transition, only some water desorption. In order to observe equation (2), oxygen molecules are needed.

The existence of $\mathrm{O^-_{2(s)}}$ species in equation (2) has been identified on $\mathrm{Au/TiO_2}$ by the isotope technique by Iwasawa et al. [49,50] and by ESR on a system containing $\mathrm{CeO_2}$ support [54]. We suggest, therefore, that reactions (1) and (2) occur along the perimeter of the gold/iron oxide interface because the XPS results show that FeO species are created when after the oxidation the gold particles are partially covered by support species. This is a possible pathway for creating active oxygen species available for the CO oxidation. One could, however, reject this assumption on the basis that on pure support this process could take place, but the lack of reaction would indicate only the absence of chemisorbed CO. Structural investigations performed above clearly show the change which occurred in the presence of gold.

The second problem is the CO activation. It is well known that CO adsorption on gold is weak and reversible [48]. On the other hand, it is also well known that small gold particles are electron deficient [28], thus, gold atoms alone are not suitable for CO chemisorption. However, the highly positive neighborhood (oxygen vacancies) helps the $\mathrm{O_2}$ adsorption, the $\mathrm{O^-_{2(s)}}$ species formed in reaction (2) interact either with the vacancy formed in the vicinity of the gold particles transferring charge to the gold surface due to the electrons being delocalized. It results in an increase in the metallic character of Au (see small, definite 0.4 eV decrease in the Au $4f_{7/2}$ BE):

$$\mathrm{Au^{\delta+}} \overset{\delta e^-}{\longleftrightarrow} \mathrm{O^-_{2(s)}} \overset{\delta e^-}{\longleftrightarrow} \square \quad (3)$$

The charge increase results in the formation of $\mathrm{Au^{\delta-}}$ species which has been assumed by Boccuzzi et al. [51]. Increased electron density on the surface of the gold particles increasing the metallic character of gold is necessary to activate CO molecules in the presence of oxygen, consequently increased electron density on gold results in an enhanced CO adsorption by the increase of backdonation from the gold d bands to the $2\pi^*$ orbital of the CO molecule according to the Blyholder mechanism [52]. The backdonation weakens the C–O bond strength resulting in activated CO molecules which react with the activated oxygen surrounding the gold particles and formed in equation (2), finally causing the higher catalytic activity.

There are several reasons why we assume the presence of the $\mathrm{O_2^-}$ species molecule during the transformation. First, there must be electron transfer from the support to the gold mediated by the $\mathrm{O_2^-}$ surface species even after oxidation. Furthermore, even in spite of the oxidative treatment a small fraction of the $\mathrm{Fe^{3+}}$ ions around the gold particles are transformed to $\mathrm{Fe^{2+}}$. Based on the electron transfer suggested, this should not be a direct transfer from the support to the gold, because if it were so, we would expect this to be the case also in the as prepared sample. This is, however, not visible. Second, on a support like iron oxide the oxygen is adsorbed mainly in the form of $\mathrm{O_2^-}$ species [47] which could result in the $\mathrm{Fe^{2+}} \rightleftharpoons \mathrm{Fe^{3+}} + \mathrm{e^-}$ transition. Third, in a recent study Iwasawa et al. [49,50] estabilished, that in the CO oxidation negatively charged oxygen molecule has a crucial role. We suppose that in the case of the oxidation treatment this molecule can be produced and beyond its effect on the gold electronic state, it could also take part in the CO oxidation. Fourth, in case of NiO it was estabilished that the highest eV value of the O 1s peak could be assigned to a peak with excess oxygen on the surface which is able to coordinate with several $\mathrm{Ni^{2+}}$ and $\mathrm{Ni^{3+}}$ species resulting in the high positive ambient and consequently, in the high BE value [53]. According to this we also explain the 535.2 eV for the O 1s peak with the presence of this kind of oxygen. Furthermore, if we consider that this oxygen molecule adsorbed in the vicinity of the $\mathrm{Au^{\delta+}}$ where we assume the $\mathrm{Fe^{2+}} \leftrightarrow \mathrm{Fe^{3+}} + \mathrm{e^-}$ transformation, one can see how much positively charged ions are present in this area and can cause the strongly positively charged ambient causing the high BE value. The scenario on the effect of the oxidation treatment is presented in scheme 1.

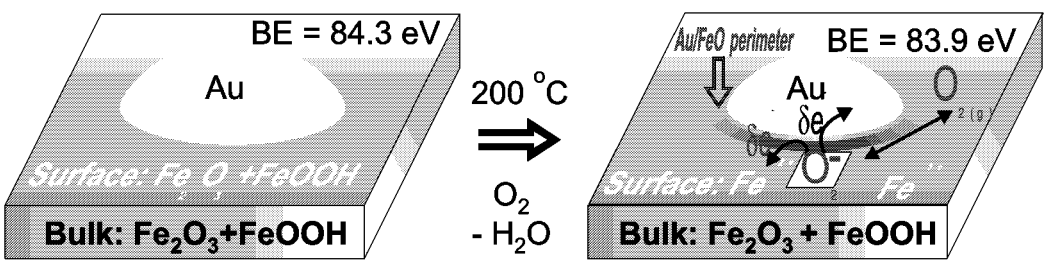

Scheme 1. Proposed mechanism for the effect of the oxidation treatment on the 1% $\mathrm{Au/FeO_x}$ catalyst prepared by coprecipitation.

After reduction the XPS peaks of FeO(OH) disappear and we are unable to detect the presence of goehtite by electron diffraction. According to this, in aggreement with the presence of the OH peak in the XPS spectrum, and the appearance of the peak of FeO and adsorbed water we assume that almost all the FeO(OH) species, which were previously present, transformed during the treatment:

$$2\mathrm{FeO(OH)} + \mathrm{H_2} \rightarrow 2\mathrm{FeO} + \square + 2\mathrm{H_2O} \qquad (4)$$

In reaction (4) the same oxygen vacancies are produced as after the oxidation, but the absence of the 535.2 eV O 1s peak and the low catalytic activity could be due to the absence of the O_2^- species which is, of course, a consequence of the absence of oxygen molecules. However, the reduced sample has high catalytic activity as compared to that observed in the as prepared state, because after reductive treatment the active sites are still present on the surface and they are able to activate the O_2 molecules presented in the reactant mixture resulting in catalytic activity.

It is also important to discuss the catalytic activity of the as prepared sample. As is shown in figure 9 the activity of the sample is negligible at the beginning of the reaction, however, after 30 min it increases to the level of the reduced sample. We explain this with the possible transformation of the support during the reaction caused by the oxygen present in the reactant mixture. At the beginning only the Fe^{3+} ions and gold particles are detected in the catalyst and only a few active sites are supposed to be present. The presence of these active sites at the beginning explains also the Au metallic state appeared already in the as prepared sample as well. During reaction, based on our hypothesis put forward in equation (1), the Fe^{3+} phase is able to transform with the help of oxygen molecules resulting in more active sites for the reaction and resulting in the gradually increasing catalytic activity.

5. Conclusions

In case of a low metal containing Au/Fe_2O_3 catalyst prepared by a coprecipitation method we obtained the same results that we had received for a model $Au/FeO_x/SiO_x$ catalyst [28]. This fact confirms our previous findings. To sum up our recent results the following conclusions can be drawn:

(i) To reach high activity in the CO oxidation a change in the size and in the oxidation state of the metallic gold particles are not needed, but an electronic interaction between the gold particles and the support is required.

(ii) The most active sample is the oxidized one in which the gold is in metallic state and the FeO_x support contains Fe_2O_3 in hematite phase, and also contains FeO and FeO(OH). The electron diffraction pattern of this sample revealed the presence of goethite which is the orthorhombic form of the FeO(OH).

(iii) After reducing the sample the maghemite-c phase of Fe_2O_3 appeared, furthermore, there is a significant decrease in activity. The oxidation state and the size of the metallic gold particles did not change during this treatment, either.

(iv) Our hypothesis concerning the effect of oxidation fits well with the results that we obtained and it explains the components identified on the catalyst at the different stage of the treatments and also the variation of the catalytic activities.

Acknowledgement

The authors are indebted to the Hungarian Academy of Sciences for financial support. The work is used for partial fulfilment of Ph.D. work of DH. The authors are grateful to Dr. Z. Schay and to E. Zsoldos for valuable discussions.

References

[1] J.C. Bailar, in: *Comprehensive Inorganic Chemistry*, Vol. 1 (Pergamon, New York, 1973) p. 129.
[2] D.I. Hagen and G.A. Somorjai, J. Catal. 41 (1976) 466.
[3] J.W.A. Sachtler, M.A. van Hove, J.P. Biberian and G.A. Somorjai, Phys. Rev. Lett. 45 (1980) 1601.
[4] G.C. Bond, Gold Bull. S1 (1972) 11.
[5] G.C. Bond and D.T. Thompson, Catal. Rev. Eng. Sci. 41 (1999) 319.
[6] D.Y. Cha and G. Parravano, J. Catal. 18 (1970) 200.
[7] G. Parravano, J. Catal. 18 (1970) 320.
[8] J. Schwank, S. Galvagno and G. Parravano, J. Catal. 63 (1980) 415.
[9] S. Galvagno and G. Parravano, J. Catal. 55 (1978) 178.
[10] M. Haruta, N. Yamada, T. Kobayashi and S. Iijima, J. Catal. 115 (1989) 301.
[11] M. Haruta, Catal. Today 36 (1997) 153.
[12] A. Ueda, T. Oshima and M. Haruta, Appl. Catal. B 12 (1997) 81.
[13] H. Sakurai and M. Haruta, Catal. Today 29 (1996) 361.
[14] M. Haruta, A. Ueda, S. Tsubota and R.M. Torres Sanches, Catal. Today 29 (1996) 443.
[15] D. Andreeva, T. Tabakova, V. Idakiev, P. Christov and R. Giovanoli, Appl. Catal. A 169 (1998) 9.
[16] S. Tsubota, D.A.H. Cunningham, Y. Bando and M. Haruta, in: *Preparation of Catalysts*, Vol. 6, eds. G. Poncelet, P. Grange and B. Delmon (Elsevier, Amsterdam, 1995) p. 22.
[17] M. Haruta, Catal. Surv. Jpn. 1 (1997) 61.
[18] A.S. Eppler, G. Rupprechter, L. Guczi and G.A. Somorjai, J. Phys. Chem. B 101 (1997) 9973.
[19] D. Guillemot, M. Polisset-Thofin, D. Bonnin, V.Yu. Borovkov and J. Fraissard, in: *Proc. 12th Int. Zeolite Conf.*, Vol. 3 (Material Research Society, 1999) p. 2079.
[20] D. Guillemot, M. Polisset-Thofin and J. Fraissard, Catal. Lett. 41 (1996) 143.
[21] D. Guillemot, V.Yu. Borovkov, V.B. Kazansky, M. Polisset-Thofin and J. Fraissard, J. Chem. Soc. Faraday Trans. 93 (1997) 3587.
[22] T.M. Salama, R. Ohnishi, T. Shido and M. Ichikawa, J. Catal. 162 (1996) 169.
[23] D.A. Cunningham, W. Vogel, H. Kageyama, S. Tsubota and M. Haruta, J. Catal. 177 (1998) 1.
[24] M. Haruta, in: Report of the Osaka National Research Institute, No. 393 (August 1999) p. 36.
[25] S. Minico, S. Sciere, C. Crisafulli, A.M. Visco and S. Galvagno, Catal. Lett. 47 (1997) 273.
[26] F.E. Wagner, S. Galvagno, C. Milone and A.M. Visco, J. Chem. Soc. Faraday Trans. 93 (1997) 3403.

[27] M. Valden, X. Lai and D.W. Goodman, Science 281 (1998) 1647.
[28] L. Guczi, D. Horváth, Z. Pászti, L. Tóth, Z.E. Horváth, A. Karacs and G. Pető, J. Phys. Chem. B 104 (2000) 3183.
[29] Y.-S. Su, M.-Y. Lee and A.D. Lin, Catal. Lett. 57 (1999) 49.
[30] E.D. Park and J.S. Lee, J. Catal. 186 (1999) 1.
[31] N.M. Gupta and A.K. Tripathi, J. Catal. 187 (1999) 343.
[32] A.K. Tripathi, V.S. Kamble and N.M. Gupta, J. Catal. 187 (1999) 332.
[33] Y. Iizuka, T. Tode, T. Takao, K. Yatsu, T. Takeuchi, S. Tsubota and M. Haruta, J. Catal. 187 (1999) 50.
[34] J.-D. Grunwaldt, M. Maciejewki, O.S. Becker, P. Fabrizioli and A. Baiker, J. Catal. 186 (1999) 458.
[35] G. Molnár, T. Belgya, L. Dabolczi, B. Fazekas, Zs. Révay, Á. Veres, I. Bikit and Z. Kiss, J. Radioanal. Nucl. Chem. (1997) 111.
[36] N.A. Boldyreva and V.K. Yatsiminsky, in: *Proc. 10th Int. Congr. Catal.*, Part C, eds. L. Guczi, F. Solymosi and P. Tétényi (Akadémiai Kiadó, Budapest, 1993) p. 2621.
[37] B.T. Upchurch, E.J. Kielin and D.E. Schryer, Catal. Lett. 31 (1995) 153.
[38] M. Haruta, S. Tsubota, T. Kobayashi, H. Kageyama, M.J. Genet and B. Delmon, J. Catal. 144 (1993) 175.
[39] S.D. Lin, M.A. Bollinger and M.A. Vannice, Catal. Lett. 17 (1993) 245.
[40] M. Haruta, T. Kobayashi, H. Sano and N. Yamada, Chem. Lett. (1987) 405.
[41] A.M. Visco, F. Neri, G. Neri, A. Donato, C. Milone and S. Galvagno, PCCP 1 (1999) 2869.
[42] W.S. Epling, G.B. Hoflund, J.F. Weaver, S. Tsubota and M. Haruta, J. Phys. Chem. B 100 (1996) 9929.
[43] Z. Zsoldos, Z. Schay and L. Guczi, Surf. Interface Anal. 12 (1988) 257.
[44] L. Borkó, I. Nagy, Z. Schay and L. Guczi, Appl. Catal. A 147 (1996) 95.
[45] R.T. Sanderson, *Chemical Periodicity* (Reinhold, New York, 1960).
[46] V.I. Nefedov, D. Gati, B.F. Dzhurinskii, N.P. Sergurhin and V.Ia. Salyn, Zh. Neorg. Chim. 20 (1975) 2307.
[47] A. Bielanski and J. Haber, *Oxygen in Catalysis* (Dekker, New York, 1991).
[48] M.A. Bollinger and M.A. Vannice, Appl. Catal. B 8 (1996) 417.
[49] H. Liu, A.I. Kozlov, A.P. Kozlova, T. Shido, K. Asakura and Y. Iwasawa, PCCP 1 (1999) 2852.
[50] H. Liu, A.I. Kozlov, A.P. Kozlova, T. Shido, K. Asakura and Y. Iwasawa, J. Catal. 185 (1999) 252.
[51] F. Boccuzzi, A. Chiorino, M. Manzoli, D. Andreeva and T. Tabakova, J. Catal. 188 (1999) 176.
[52] G. Blyholder, J. Phys. Chem. 68 (1964).
[53] J. Finster, P. Lorenz, F. Fievet and M. Figlarz, in: *Proc. 9th Symp. Reactivity Solids*, 1980, Vol. 1 (Elsevier, New York, 1981) p. 391.
[54] A. Martinez-Arias, J.M. Coronado, R. Cataluna, J.C. Conessa and J. Soria, J. Phys. Chem. B 102 (1998) 4357.